Effects of varying compressive biaxial strain on the hydrogen uptake of thin vanadium (001) layers

1999 J. Phys.: Condens. Matter 11 6669

(http://iopscience.iop.org/0953-8984/11/35/305)

J. Phys.: Condens. Matter **11** (1999) 6669–6677. Printed in the UK PII: S0953-8984(99)03697-8

Effects of varying compressive biaxial strain on the hydrogen uptake of thin vanadium (001) layers

G Andersson†, P H Andersson† and B Hjörvarsson‡§

† Department of Physics, Uppsala University, Box 530, SE-751 21 Uppsala, Sweden
‡ Department of Physics, Royal Institute of Technology, SE-100 44 Stockholm, Sweden

Received 23 April 1999

Abstract. The hydrogen uptake of asymmetric Fe/V (001) superlattices with $L_{Fe}/L_V = 3/16$ monolayers and 3/10 monolayers was investigated by resistometric methods. The hydrogen distribution and the enthalpy of solution were simulated using a diffusion model and calculated H–H interaction energies. It was found that the strain state of the V lattice strongly influenced the H–H interaction. The hydrogen-depleted interface region in the V layers was populated at lower concentrations than in previously studied symmetric samples, which implied that the energy difference between interior and interface regions was lowered. The V–H binding energy was found to be up to 60 meV higher than in the symmetric superlattices.

1. Introduction

It has been observed in previous studies on the hydrogen uptake of vanadium in Mo/V and symmetric ($L_{Fe} = L_V$) Fe/V (001) superlattices that the thermodynamics is strongly dependent on the biaxial (in-plane) strain state of the V lattice [1–4]. This was theoretically predicted in the early 1970s [5]. In Mo/V (001), where the biaxial strain is tensile, the hydrogen–hydrogen interaction is attractive [4], whereas in symmetric Fe/V (001) superlattices it is repulsive except at very low concentrations [1] due to the compressive in-plane strain. In Fe/V (001) superlattices with $L_{Fe} < L_V$ the vanadium lattice will be less strained than in the symmetric samples.

In the present investigation superlattices with $L_{Fe}/L_V = 3$ ML/16 ML and 3 ML/10 ML are under consideration. In the thickness range including these samples and the previously studied symmetric samples ($L_{Fe} = L_V \leqslant 14$ ML) the compressive in-plane strain in the V layers is proportional to the ratio between the individual layer thicknesses of iron and vanadium. One question that is addressed is whether the Fe layer thickness affects the H uptake only by altering the strain state of the vanadium, or whether there are additional effects from a change in the charge transfer from Fe to V at the interfaces [3]. Hence, the extent of the hydrogen-depleted region close to each interface may depend on the relative amount of iron.

For the interpretation of thermodynamic data a simple theoretical model, which involves the hydrogen–hydrogen interaction energies, of the hydrogen distribution in the V layers and the related changes in energy has been employed. It will be shown that this model reproduces the enthalpy data, and that it can be used to estimate the repulsive interaction energies at intermediate concentrations where detailed total-energy calculations are too time consuming.

§ Author to whom any correspondence should be addressed.

0953-8984/99/356669+09$30.00

Fe/V superlattices with varying proportions between the constituents have shown great variation in magnetic properties in recent measurements [6–8]. In (001) superlattices with 3 ML of Fe and 12–15 ML of V it was found that the magnetic coupling between the iron layers, which is antiferromagnetic for 13–14 ML of V, could be switched by introducing hydrogen into the vanadium layers [9]. In the samples with 3 ML Fe/15 ML V the coupling changed from ferromagnetic to antiferromagnetic and back to ferromagnetic on introduction of hydrogen up to an average concentration of $H/V \approx 0.05$. In order to be able to control the degree of switching it is vital to have some knowledge of the pressure–composition–temperature characteristics of the hydrogen uptake of these superlattices. The results of the present investigation will supply a major part of this knowledge.

2. Experimental details

The samples used in the experiments were epitaxial Fe/V (001) superlattices grown on MgO substrates by dc magnetron sputtering as described previously [1, 10]. The nominal compositions were [3 ML Fe/16 ML V]$_{30}$ and [3 ML Fe/10 ML V]$_{40}$, respectively (total thicknesses 86 nm and 78 nm). Both samples were covered with 3 nm Pd for the hydrogen absorption measurements. The samples will be referred to as 3/16 and 3/10, respectively, reflecting the ratio L_{Fe}/L_V of the individual layer thicknesses.

The gas loading equipment described in previous papers [1] was used. This is an UHV system with a four-point set-up for resistivity measurements. Partial pressures of residual gases other than hydrogen are below 10^{-11} mbar. The measurement procedure was the same as described previously [1], i.e. increasing the hydrogen pressure in steps at constant temperature while measuring the resistivity change. The temperatures used in the measurements were 30, 45, 80, 100, 125, 150 and 200 °C, and hydrogen pressures were in the range 0.02–8000 mbar.

3. Results

The sample structure was investigated before and after the hydrogen loading using x-ray diffraction. An example of low-angle and high-angle data for the 3/16 sample is shown in figure 1. No changes, within experimental uncertainties, of the structural quality were observed after the completed hydrogen cycling. The average out-of-plane lattice parameter obtained from the diffraction data was 0.298(1) nm for the 3/16 sample, and 0.2962(1) nm for the 3/10 sample. The measured chemical modulation wavelengths agreed with the nominal values. The samples are of the same high quality as those described in references [1, 9, 10], i.e. the individual layers are well defined (the interface roughness is ±1 monolayer) and of constant thickness throughout the samples. The previously described neutron reflectivity measurements on similar samples [9] show that the conditions at the interfaces are not altered by repeated hydrogen loading.

The pressure–resistivity isotherms for both superlattices are shown in figure 2. The relations between the measured $\Delta\rho/\rho_{20\,^\circ C}$ and the reduced concentration c/c_{max} in the interior of each vanadium layer (i.e. the region that is not hydrogen-depleted) were found to be

$$\begin{aligned} \Delta\rho/\rho_{20\,^\circ C} &= 1.32(6)c/c_{max} - 0.51(6)c/c_{max}^2 \\ \Delta\rho/\rho_{20\,^\circ C} &= 1.22(3)c/c_{max} - 0.61(3)c/c_{max}^2 \end{aligned} \qquad (1)$$

for the 3/16 and the 3/10 samples, respectively. The derivation was based on the following assumptions:

(a) The relations are of the same form as for the symmetric samples [1]:

$$\Delta\rho/\rho_{20\,^\circ C} = k_1 c/c_{max} - k_2 c/c_{max}^2. \qquad (2)$$

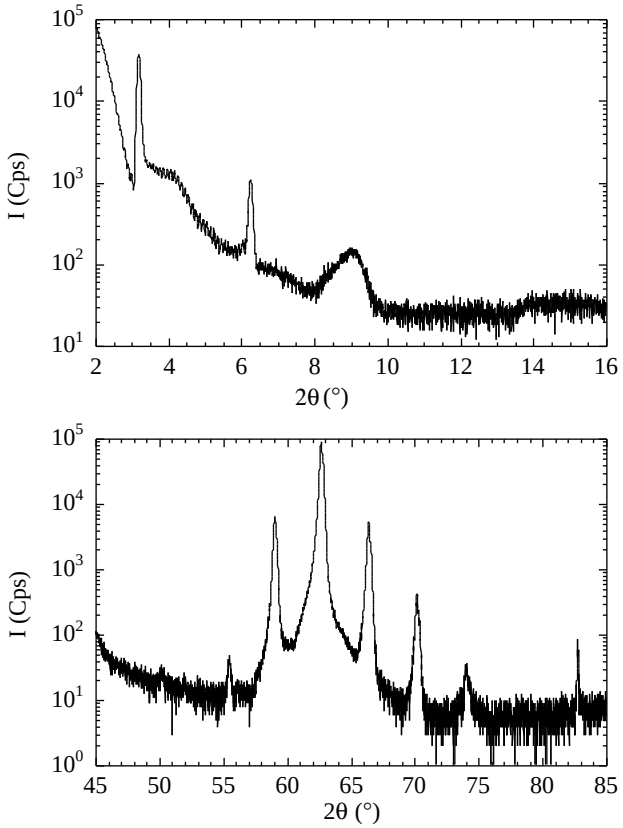

Figure 1. Low- and high-angle x-ray diffraction data for the 3/16 sample.

(b) The points of inflection in the curves of $\ln\sqrt{p}$ versus $\Delta\rho/\rho_{20\,^\circ\mathrm{C}}$, which are temperature independent as for the symmetric superlattices [1], correspond as in that case to an interior concentration of $c/c_{\max} = 1/6$. These points give the critical concentrations for a phase transition. For the 3/10 sample the average position of the point of inflection is $\Delta\rho/\rho_{20\,^\circ\mathrm{C}} \approx 0.186(4)$, and for the 3/16 sample the corresponding value is $\Delta\rho/\rho_{20\,^\circ\mathrm{C}} \approx 0.206(9)$.

(c) The maximum observed at 30 °C for the 3/16 sample ($\Delta\rho/\rho_{20\,^\circ\mathrm{C}} = 0.810\,20(5)$) corresponds to the maximum interior concentration, $c/c_{\max} = 1$. For the 3/10 sample, the same assumption was made about the maximum value measured at 30 °C ($\Delta\rho/\rho_{20\,^\circ\mathrm{C}} = 0.607\,45(5)$), although no sign of subsequent decrease in $\Delta\rho/\rho_{20\,^\circ\mathrm{C}}$ was observed. However, the 30 °C and 45 °C isotherms tend towards the same value. In the symmetric samples, the maximum in $\Delta\rho/\rho_{20\,^\circ\mathrm{C}}$ was temperature independent [1].

The raw pressure–resistivity data were used to calculate the enthalpy and entropy of solution at constant resistivity change, using the van't Hoff equation

$$\ln\sqrt{\frac{p}{p_0}} = \frac{\Delta\overline{H}_{\mathrm{H}}}{k_{\mathrm{B}}T} - \frac{\Delta\overline{S}_{\mathrm{H}}}{k_{\mathrm{B}}} \tag{3}$$

and equation (1) was used to convert resistivity change into reduced interior concentration. The resulting data are shown in figures 3 (enthalpy of solution) and 4 (entropy of solution).

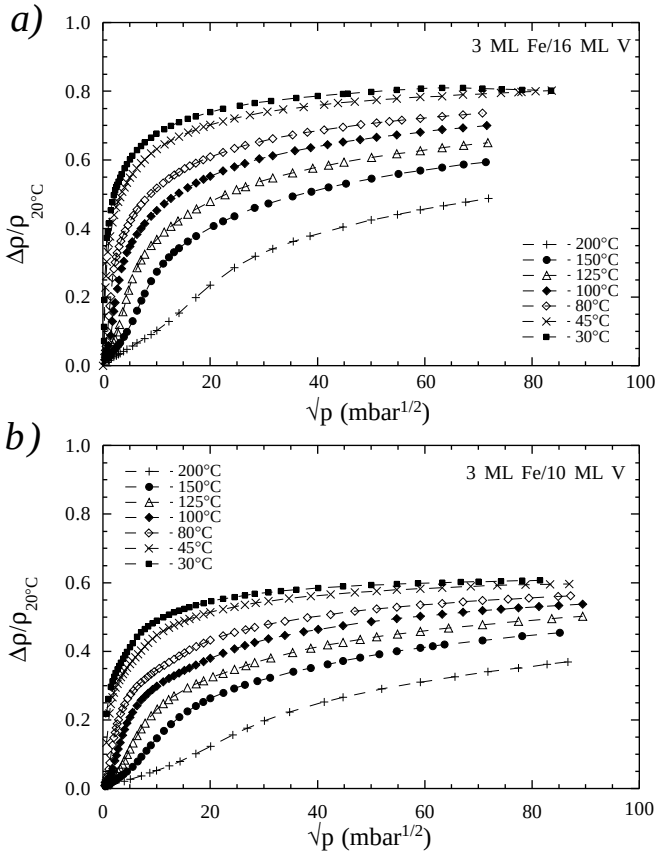

Figure 2. Pressure–resistivity isotherms for (a) $L_{\mathrm{Fe}}/L_{\mathrm{V}} = 3/16$ ML and (b) $L_{\mathrm{Fe}}/L_{\mathrm{V}} = 3/10$ ML.

These figures also include the corresponding data for the symmetric superlattices [1]. To make unambiguous comparison possible, $c/c_{\max}$ is used for the abscissa in all subplots. For the time being, $c_{\max} = 1$ is assumed for the asymmetric superlattices, whereas for the symmetric samples calibration measurements of the concentration have confirmed this value. In figure 3 the curves obtained from the calculations described below are included as lines.

4. Discussion

The $\Delta\overline{H}_{\mathrm{H}}$ and $\Delta\overline{S}_{\mathrm{H}}$ values in figures 3 and 4 are not affected even if the assumption $c_{\max} = 1$ does not hold for the 3/10 and 3/16 samples, as the only effect would be a rescaling of the absolute interior concentration scale. One fact that does support the present absolute resistivity–concentration relations is that the decrease in $\Delta\overline{H}_{\mathrm{H}}$ (i.e. attractive H–H interaction) ends at $c/c_{\max} \approx 0.1$, as for the symmetric samples.

The equipment necessary to determine the strain experimentally was not available during this series of measurements. However, the in-plane lattice parameter, $a_{\parallel}$, can be assumed to vary linearly with the ratio $L_{\mathrm{Fe}}/L_{\mathrm{V}}$. From the experimental values for bulk V ($L_{\mathrm{Fe}}/L_{\mathrm{V}} = 0, a_0 = 0.302\,74$ nm [10]) and for the symmetric (001) superlattices ($L_{\mathrm{Fe}}/L_{\mathrm{V}} = 1$,

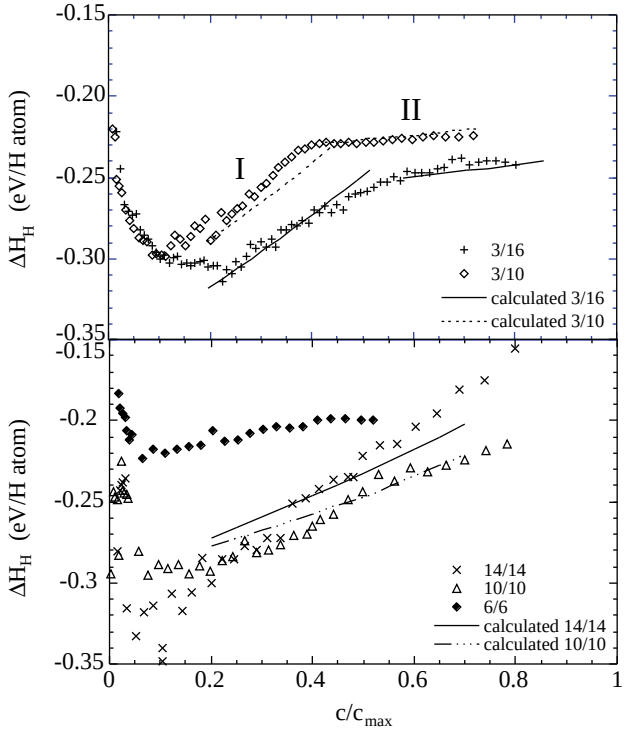

Figure 3. Enthalpy of solution versus interior reduced concentration for the asymmetric (top) and symmetric (bottom) [1] superlattices, including calculated values as described in the text. The labels refer to the ratio $L_{\mathrm{Fe}}/L_{\mathrm{V}}$ of each sample. Note that with the present resistivity–concentration relations, the maximum concentration is 1 for all samples.

$a_{\parallel} = 0.2915$ nm, $a_{\perp} = 0.3053$ nm [10]), one obtains the relation

$$a_{\parallel} = a_0 - 0.011\frac{L_{\mathrm{Fe}}}{L_{\mathrm{V}}}. \tag{4}$$

Using this equation the in-plane lattice parameters of the 3/10 and 3/16 samples are 0.2994 nm and 0.3006 nm, respectively. From the lattice parameters of the symmetric samples a superlattice Poisson ratio can be obtained, and thus the out-of-plane lattice parameters (0.3035 nm and 0.3032 nm). These calculated lattice parameters of Fe and V yield average out-of-plane parameters of 0.297 nm and 0.299 nm, respectively, which are close to those obtained from x-ray diffraction (figure 1).

The unit-cell volumes of both V and Fe increase with decreasing relative amount of Fe. The volume difference of V between the symmetric and asymmetric samples is approximately 5%. Assuming that the electronic structure is not significantly altered, the interstitial electron density (IED) has decreased by the same percentage. An estimate of the change in H–V binding energy, δE_{B}, with average IED change, $\delta\overline{n}_0$, is given by [1, 11]

$$\delta E_{\mathrm{B}}\ (\mathrm{eV}) = (796\overline{n}_0 + 20.9)\delta\overline{n}_0. \tag{5}$$

With $\overline{n}_0 = 0.03$ au^{-3} [11] and a 5% decrease in IED the binding energy in the asymmetric samples increases by 67 meV as compared to the symmetric samples.

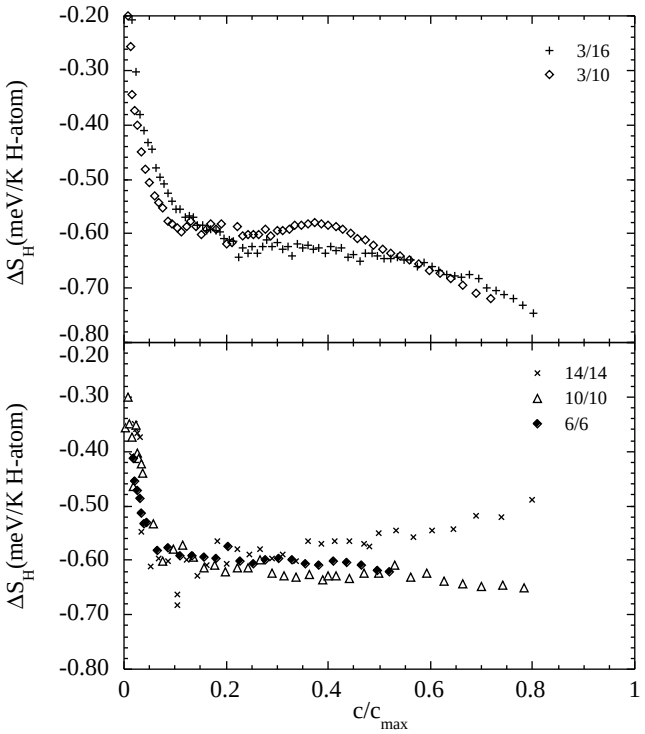

Figure 4. Entropy of solution versus interior reduced concentration for the asymmetric (top) and symmetric (bottom) [1] superlattices.

4.1. Enthalpy and entropy data

In the low-concentration region $\Delta\overline{H}_{\mathrm{H}}$ and $\Delta\overline{S}_{\mathrm{H}}$ exhibit the same qualitative $c/c_{\max}$ dependence as in the symmetric samples. We thus have attractive H–H interaction in the xy-plane, i.e. the film plane, mediated by lattice expansion in the out-of-plane (z-) direction [1].

In the symmetric 6/6 ML sample the infinite-dilution limit of $\Delta\overline{H}_{\mathrm{H}}$ is -0.16 eV/H atom (figure 3). The data for the 10/10 and 14/14 samples also shown in this figure are more difficult to extrapolate to zero concentration, but -0.18 eV/H atom is a reasonable value for both. For 3/10 and 3/16 the value is -0.22 eV/H atom, i.e. roughly 40–60 meV lower than for the symmetric samples. The V–H binding energy increase of 67 meV estimated above agrees rather well with this value.

At $c/c_{\max} \approx 0.1$ there is a minimum in $\Delta\overline{H}_{\mathrm{H}}$ for both 3/10 and 3/16, as well as for the symmetric samples. At the minimum the repulsive interaction, caused by the limited possibility of expanding the lattice to accommodate more H atoms, and the formerly dominating attractive interaction are in balance. The repulsive interaction then takes over at lower concentrations in the 3/10 sample than in 3/16. The entropy of solution decreases strongly for $c/c_{\max} < 0.1$, indicating increasing order.

In the intermediate-concentration region ($c/c_{\max} = 0.1$–0.4 for $L_{\mathrm{Fe}}/L_{\mathrm{V}} = 3/10$ and $c/c_{\max} = 0.2$–0.6 for $L_{\mathrm{Fe}}/L_{\mathrm{V}} = 3/16$, respectively) the net H–H interaction is repulsive. The symmetric and asymmetric samples are still similar in this concentration region. There is short-range hydrogen order in the xy-plane and correlation in the z-direction throughout

each V layer, resulting in what was previously denoted as a 'two-dimensional liquid' [1]. In accordance, $\Delta\overline{S}_{\mathrm{H}}$ is roughly constant in this concentration region, suggesting a certain degree of remaining disorder.

At concentrations above $c/c_{\max} \approx 0.4$ for 3/10 and $c/c_{\max} \approx 0.6$ for 3/16 the slope of $\Delta\overline{H}_{\mathrm{H}}$ is close to zero and $\Delta\overline{S}_{\mathrm{H}}$ starts to decrease from the plateau values of approximately -0.6 meV K^{-1}/H atom. The most plausible interpretation, suggested by comparison with the data for the 6/6 ML sample, is that H atoms are populating the third monolayer from each interface to a larger extent. The H atoms are forced to order in this monolayer, resulting in a 'freezing' of the two-dimensional liquid and decreasing $\Delta\overline{S}_{\mathrm{H}}$. The repulsive H–H interaction simultaneously decreases considerably.

In the symmetric samples the hydrogen atoms were found to occupy octahedral z-sites (O_z) [1]. An alternative reason for the behaviour of $\Delta\overline{H}_{\mathrm{H}}$ is population of additional sites other than O_z. This would then be caused by the lower degree of compressive strain, as a slightly smaller tetragonal distortion than in the symmetric samples could make other sites available. This possibility is supported by the $\Delta\overline{S}_{\mathrm{H}}$ data. However, the onset of almost constant $\Delta\overline{H}_{\mathrm{H}}$ would then be at a lower concentration in the 3/16 sample than in the 3/10 sample, as the vanadium lattice is less distorted for the smaller $L_{\mathrm{Fe}}/L_{\mathrm{V}}$ ratio. This is not observed.

4.2. Theoretical model

For the calculation of the H–H interaction energies it was assumed that the system could be described by a simple Ising model where the total energy is a sum of atomic terms and interaction terms. The energy was calculated for a number of different configurations with H at octahedral sites where the numbers of nearest, next-nearest and third-nearest neighbours differed. Then the atomic and interaction energies were fitted to the total energies. This gave the H–H interaction energy per added hydrogen atom.

As the elastic interaction depends on the concentration the calculations were restricted to one H/V value. Configurations with $\mathrm{H/V} = 0.5$ were chosen, as this was close to the concentrations of interest ($\mathrm{H/V} = 0.4$–0.6) and allowed a relatively small supercell to be used. The experimental values of the in-plane and out-of-plane lattice parameters were used.

The desired resolution of the interaction energies was of the order of meV. To achieve this resolution a full-potential linear augmented-plane-wave (FP-LAPW) method [12, 13] based on density functional theory (DFT) [14, 15] in the local density approximation (LDA) [16] was used for the calculation of interaction energies. For the sampling of the $\boldsymbol{k}$-space a Fermi–Dirac temperature smearing was used for the integration of the Brillouin zone as this method gives a reliable result within reasonable time. The calculations were well converged with respect to the number of plane waves and $\boldsymbol{k}$-points.

In order to see whether the third monolayer from the interface could be populated in these samples, simulations of the hydrogen distribution in the V layers were performed. In these simulations the H–H interactions between nearest, next-nearest and third-nearest neighbours (ϵ_1, ϵ_2 and ϵ_3, respectively) were used. For a hydrogen atom in an O_z site in a tetragonally distorted lattice the nearest neighbours are in the next monolayer in the $\langle 111 \rangle$ directions, the next-nearest neighbours are in the same monolayer in the (100) and (010) directions and the third-nearest neighbours are in the second monolayer in the (001) direction, as $a_\perp > a_\parallel$.

The energy barrier for diffusion from monolayer i to the adjacent layers is lowered by an amount ΔE_i compared to the infinite-dilution value:

$$\Delta E_i = 4\epsilon_1(c_{i-1} + c_{i+1}) + 2\epsilon_2 c_i + \epsilon_3(c_{i-2} + c_{i+2}) \tag{6}$$

where c_j is the H/V atomic ratio in layer j. Using this in a simple diffusion model gave the

interface and interior concentrations for a fixed value of the interface–interior energy difference. The total energy change per H atom was then calculated as

$$E = \frac{1}{2N}\sum_{i=1}^{N} 4\epsilon_1(c_{i-1} + c_{i+1}) + 4\epsilon_2 c_i + \epsilon_3(c_{i-2} + c_{i+2}) \tag{7}$$

where N is the number of possibly populated V monolayers, i.e. $N = N_V - 4$ if the third layer from each interface and the interior layers are included. A plot of E versus interior concentration should have the same slope as the experimental $\Delta\overline{H}_H$ curve. For high concentrations in both samples this is found when using equation (7) with $N = N_V - 4$ and the interaction energies $\epsilon_1 = 4.20$ meV/H atom, $\epsilon_2 = 7.59$ meV/H atom and $\epsilon_3 = 8.73$ meV/H atom obtained from the calculations for H/V = 0.5, as seen in region II in figure 3. This indicates that the model is applicable to the problem.

The H–H interaction energies for H/V = 0.5 could not reproduce the section of the $\Delta\overline{H}_H$ curves corresponding to concentrations between 0.2 and 0.4 (0.6 for the 3/16 sample). In this case a comparison with the symmetric superlattices was made. In the 6/6 ML sample the hydrogen atoms are distributed in the innermost two layers. Thus the positive slope in $\Delta\overline{H}_H$ can be regarded as an estimate of the in-plane interaction energy (ϵ_2). In the 10/10 ML sample there are four populated layers, which implies that the difference in slope between 10/10 and 6/6 yields the interaction energy with the neighbours in the next monolayer (ϵ_1), and analogously an estimate of the energy ϵ_3 is obtained from the 14/14 data. The enthalpy curves for the 10/10 and 14/14 ML samples at concentrations between 0.2 and 0.7 were successfully reproduced using the models above and $\epsilon_1 = 22$ meV/H atom, $\epsilon_2 = 12.5$ meV/H atom and $\epsilon_3 = 60.8$ meV/H atom, as shown in the lower panel of figure 3.

For the asymmetric samples the interaction energies above cannot be applied directly, as the strain states differ. Instead they were estimated in the following way. The difference in slope of $\Delta\overline{H}_H$ between the 3/10 sample and the 10/10 sample contains the changes in both ϵ_1 and ϵ_2. If it is assumed that $\Delta\epsilon_1$ is negligible compared to $\Delta\epsilon_2$ and that $\Delta\epsilon_3 = -\Delta\epsilon_2$ due to the lattice response, $\epsilon_1 \approx 22$ meV/H atom, $\epsilon_2 \approx 50.2$ meV/H atom and $\epsilon_3 \approx 23.1$ meV/H atom are obtained. Furthermore, it is assumed that the interaction energies are the same within the uncertainties in the 3/10 and 3/16 samples. The curves in region I of figure 3 were calculated using these values and $N = N_V - 6$ in equation (7), i.e. no population of the interface region.

5. Summary and conclusions

The hydrogen uptake of Fe/V (001) superlattices with $L_{Fe}/L_V = 3/10$ and 3/16 monolayers was investigated. At low concentrations the H–H interaction was found to be attractive and at intermediate concentrations it was repulsive, which is the same behaviour as was observed previously for symmetric Fe/V (001) superlattices. At higher concentrations the repulsive interaction is balanced by an attractive interaction, resulting in almost no net H–H interaction. This is accompanied by decreasing entropy, suggesting a transition from a two-dimensional liquid at intermediate concentrations to a more ordered state. The most plausible reason for this is that hydrogen atoms occupy the first monolayer of the interface region. It is concluded that the energy difference between the third and fourth monolayers from the Fe/V interface is smaller than the 92 meV observed for the symmetric superlattices, and that the H–H interaction energy is strongly influenced by the strain state. The V–H binding energy is increased by 40–60 meV due to the changes in vanadium unit-cell volume.

Acknowledgments

Financial support from the Swedish Natural Science Research Council (NFR) is gratefully acknowledged. Special thanks are also due to Dr P Isberg for the growth of high-quality samples and to Dr L Nordström for fruitful discussions.

References

[1] Andersson G, Hjörvarsson B and Isberg P 1997 *Phys. Rev.* B **55** 1774
[2] Hjörvarsson B, Andersson G and Karlsson E 1997 *J. Alloys Compounds* **253+254** 51
[3] Hjörvarsson B, Rydén J, Karlsson E, Birch J and Sundgren J-E 1991 *Phys. Rev.* B **43** 6440
[4] Stillesjö F, Ólafsson S, Isberg P and Hjörvarsson B 1995 *J. Phys.: Condens. Matter* **7** 8139
[5] Alefeld G 1972 *Ber. Bunsenges. Phys. Chem.* **76** 746
[6] Granberg P, Isberg P, Hjörvarsson B, Nordblad P and Wäppling R 1996 *Phys. Rev.* B **54** 1199
[7] Poulopoulos P, Isberg P, Platow W, Wisny W, Farle M, Hjörvarsson B and Baberschke K 1997 *J. Magn. Magn. Mater.* **170** 57
[8] Granberg P, Isberg P, Svedberg E B, Hjörvarsson B, Nordblad P and Wäppling R 1998 *J. Magn. Magn. Mater.* **186** 154
[9] Hjörvarsson B, Dura J A, Isberg P, Watanabe T, Udovic T J, Andersson G and Majkrzak C F 1997 *Phys. Rev. Lett* **79** 901
[10] Isberg P, Svedberg E B, Hjörvarsson B, Wäppling R and Hultman L 1997 *Vacuum* **48** 483
[11] Nörskov J K 1982 *Phys. Rev.* B **26** 2875
[12] Andersen O K 1975 *Phys. Rev.* B **12** 3060
[13] Singh D J 1994 *Planewaves, Pseudopotentials and the LAPW Method* (Boston, MA: Kluwer Academic)
[14] Hohenberg P and Kohn W 1964 *Phys. Rev.* **136** B864
[15] Kohn W and Sham L J 1965 *Phys. Rev.* **140** A1133
[16] von Barth U and Hedin L 1972 *J. Phys. C: Solid State Phys.* **5** 1629